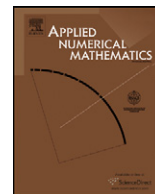




ELSEVIER

Contents lists available at ScienceDirect

Applied Numerical Mathematics

www.elsevier.com/locate/apnum

Analysis of global multiscale finite element methods for wave equations with continuum spatial scales

Lijian Jiang^{a,*}, Yalchin Efendiev^b, Victor Ginting^c^a IMA, University of Minnesota, Minneapolis, MN 55455-0134, United States^b Department of Mathematics, Texas A&M University, College Station, TX 77843-3368, United States^c Department of Mathematics, University of Wyoming, Laramie, WY 82071, United States

ARTICLE INFO

Article history:

Received 21 October 2008

Received in revised form 30 March 2010

Accepted 29 April 2010

Available online xxxx

Keywords:

Galerkin multiscale finite element

Continuum scales

Wave equations

ABSTRACT

In this paper, we discuss a numerical multiscale approach for solving wave equations with heterogeneous coefficients. Our interest comes from geophysics applications and we assume that there is no scale separation with respect to spatial variables. To obtain the solution of these multiscale problems on a coarse grid, we compute global fields such that the solution smoothly depends on these fields. We present a Galerkin multiscale finite element method using the global information and provide a convergence analysis when applied to solve the wave equations. We investigate the relation between the smoothness of the global fields and convergence rates of the global Galerkin multiscale finite element method for the wave equations. Numerical examples demonstrate that the use of global information renders better accuracy for wave equations with heterogeneous coefficients than the local multiscale finite element method.

© 2010 IMACS. Published by Elsevier B.V. All rights reserved.

1. Introduction

Over the past few decades, there has been growing interest in wave propagation in heterogeneous media. Many important problems such as earthquake motions, oceanography, medical and material sciences, and the morphology of oil and gas deposits can be understood through some use of mathematical and numerical modeling of wave propagation in heterogeneous media [5]. In the field of petroleum prospecting for example, seismic wave propagation and reflection are used to image the earth's structure [12] and to estimate the amount of hydrocarbon within certain parts of earth's crust [11]. It is now widely recognized that recoverable deposits of petroleum are increasingly difficult to locate. Moreover, the cost of drilling and extraction is becoming more expensive. Consequently, this creates a dire need for more detailed imaging of underground earth's structures. The advancement of three-dimensional data acquisition which gives way to inclusion of larger amount measurement data in the simulation processes would result in the increase of computational effort.

In addition to heterogeneity, wave propagation is also a challenging multiscale problem. Among typical length scales present in wave propagation are wave length, propagation distance, and correlation length. In some problems such as in reflection seismology, the wave can propagate over a distance significantly larger than the wave length. Furthermore, heterogeneity of the medium through which the wave moves gives a characteristic quantified by the correlation length. Taken all together, even with today's computing technology, it is virtually impossible to conduct direct simulation for wave propagation, so techniques are required to enable the solution of the problems in practice. In the case of correlation length much smaller than the wave length, the homogenization technique can be employed to estimate the effective domain with size comparable to the wave length. Some recent variation of homogenization (or upscaling) techniques for the acoustic

* Corresponding author.

E-mail addresses: lijiang@ima.umn.edu (L. Jiang), efendiev@math.tamu.edu (Y. Efendiev), vginting@uwyo.edu (V. Ginting).

wave equations that are not restricted to this requirement can be found, for example in [27,24], and [30]. Furthermore in many applications strong non-local effects are crucial and thus need to be taken into account in the simulation.

We note that in the context of flow in porous media, progress has been achieved to tackle the multiscale nature of the problems. Upscaling procedures (see [18] for reviews and discussion), and multiscale finite elements [20,8,3,1,16] have been commonly applied for this purpose and are effective in many cases. Most of these methods rely on some local calculations either in the form of effective parameters or basis functions which are then incorporated into a coarse scale formulation. In addition, the importance of global information in porous media flow has been illustrated within the context of upscaling procedures [7] and also in multiscale finite (volume) elements [1,16,23,26,27]. These studies have shown that the use of global information in the calculation of the upscaled parameters (or basis functions) can significantly improve the accuracy of the resulting coarse model. The global multiscale methods can remove the resonance error that usually exhibit themselves as the ratio between the coarse mesh size and the characteristic length scale.

We intend to extend the idea already used in porous media flow to the simulation of acoustic wave equations. The goal of this paper is to explore and analyze multiscale finite element methods for acoustic wave equations in heterogeneous media. We would like to develop approaches in the presence of strong non-local effects in the media properties. In the approaches, we assume that the solution of the wave equation smoothly depends on some global fields that can be obtained *a priori*. We discuss some distinct cases, where these global fields can be found. The calculation of global fields is an overhead in the computations. However, these global fields allow us to compute the solution on the coarse grid. Moreover, these basis functions (constructed on a coarse grid) can be repeatedly used for the computation of the solution for modified coefficients, different boundary conditions and right-hand sides. The underlying assumption for the global fields used in the paper is that there exists N ($N \geq 1$) global fields/functions $p_1(x), \dots, p_N(x)$ such that

$$\|u(t, x) - G(p_1(x), \dots, p_N(x), t)\| \leq \delta, \quad (1)$$

where $u(t, x)$ is the solution of the wave equation, and G is a function that smoothly depends on $p_i(x)$ ($i = 1, \dots, N$). We note that G does not depend on x directly and just through the x -dependence of each $p_i(x)$ ($i = 1, \dots, N$). We will provide some examples for the global functions $p_i(x)$ (see Remarks 3.1 and 3.2), and discuss the smoothness of G and the norm $\|\cdot\|$ such that the assumption (1) is satisfied. Here δ is sufficiently small and refers to a physical parameter that shows how well the solution $u(t, x)$ can be represented using the global functions $p_1(x), \dots, p_N(x)$. This assumption (1) will be used for analysis of the Galerkin Multiscale Finite Element Method (MsFEM) in Section 3.

In the paper, we focus the discussion on Galerkin MsFEM using limited global information from solution a global elliptic equation [16] for the wave equations. As a viable alternative, in Appendix A we also present a mixed MsFEM for the wave equation employing multiple global fields. We would like to note the differences between the two methods. In the first method, the basis functions for the solution $u(t, x)$ are constructed by using global fields. These basis functions are further used in the Galerkin formulation of wave equation. For the second method, basis functions for the velocity $\sigma(t, x)$ are constructed and used within mixed finite element framework. The basis functions use Neumann boundary conditions and the mixed formulation is mass conservative.

A set of numerical experiments presented in this paper reveals the improvement of accuracy of the MsFEM when some global information is taken into consideration. This is especially more significant when the media properties exhibit strong non-local features. This global MsFEM is compared to the Galerkin MsFEM that employs local basis functions (local basis functions are linear along edges of elements). We observe that the global Galerkin MsFEM performs better than those using local basis functions.

The rest of the paper is organized as follows. In Section 2, we present the problem setting. In Section 3, we discuss Galerkin MsFEM using global information. In Section 4, we show some numerical results for the Galerkin MsFEM using global information. Some conclusions are drawn in Section 5. The mixed MsFEM using information from multiple global fields is described in Appendix A.

2. Preliminaries

First, we introduce some notations which are used in the following sections. The usual Lebesgue and Sobolev spaces are denoted by $L^p(D)$, $W^{k,p}(D)$, with $\|\cdot\|_{0,D}$ and $\|\cdot\|_{0,p,D}$ being the L^2 -norm and L^p -norm for $p \neq 2$, respectively, and $\|\cdot\|_{k,D}$ and $\|\cdot\|_{k,p,D}$ being the H^k -norm and $W^{k,p}$ -norm for $p \neq 2$, respectively. The corresponding semi-norms by $|\cdot|_{k,D}$ and $|\cdot|_{k,p,D}$ are defined similarly. The time-dependent Sobolev space is equipped with norm

$$\|u\|_{W^{m,p}(0,T;X)} := \left(\int_0^T \sum_{0 \leq k \leq m} \|D_t^k u\|_X^p dt \right)^{\frac{1}{p}},$$

where X is a normed space and semi-norm

$$|u|_{W^{m,p}(0,T;X)} := \left(\int_0^T \sum_{0 \leq k \leq m} |D_t^k u|_X^p dt \right)^{\frac{1}{p}}$$

when X is a semi-norm space. If $p = 2$, we use $H^m(0, T; X)$ instead. When no ambiguity occurs, we use $W^{m,p}(X)$ to denote $W^{m,p}(0, T; X)$. The semi-norm

$$\|u\|_{\Omega_T}^2 = \|D_t u\|_{L^\infty(L^2(\Omega))}^2 + |u|_{L^\infty(H^1(\Omega))}^2$$

is often used in the stability estimate of wave equations.

An acoustic wave equation reads:

$$\begin{cases} D_{tt}u(t, x) - \nabla \cdot (a(x)\nabla u(t, x)) = f(t, x) & \text{in } \Omega_T := (0, T] \times \Omega, \\ u(x, 0) = g_0(x) & \text{in } \Omega, \\ D_t u(x, 0) = g_1(x) & \text{in } \Omega, \end{cases} \quad (2)$$

where D_t and D_{tt} respectively denote the first and second order partial derivative operator with respect to t , and $a(x)$ is a uniformly positive and bounded function in Ω representing the density of the material. This function exhibits multiscale and heterogenous features. We assume that (2) is completed with some boundary conditions.

This equation arises for example, in geophysics, electromagnetics, and seismology [29]. It is frequently observed that the spatial scales inherent in $a(x)$ cannot be clearly separated. Consideration for accuracy suggests that the heterogeneity of $a(x)$ has to be sufficiently resolved when solving (2) numerically, which can easily result in very expensive computations. While much more efficient and inexpensive in practice, standard upscaling techniques and multiscale methods employing some local information often fail to accurately transfer the fine scale information in $a(x)$ to the coarse formulation. Previous investigations (see e.g., [26,16]) indicate that appropriately taking into account some type of global information can potentially improve the accuracy of the multiscale methods. In particular, this information is determined by some global fields that the solution u smoothly depends on. In the context of the weak formulation, this global field is imbedded in the (multiscale) basis functions which in turn is used to represent the solution. Our objective is to develop multiscale methods that can capture the solution of (2) using these multiscale basis functions.

We assume that source term $f(t, x)$, initial value $g_0(x)$ and $g_1(x)$ are smooth enough, e.g., $f(t, x) \in L^2(\Omega_T)$, $g_0(x) \in H^1(\Omega)$ and $g_1(x) \in L^2(\Omega)$. To simplify presentation, we shall not write the variables t and x for the functions expressed in (1) and (2) when no ambiguity occurs. Without loss of generality, our discussion is concentrated for problems in $\Omega \subset \mathbb{R}^2$. We denote by K a generic coarse element with $h = \text{diam}(K)$, and τ_h is a quasi-uniform family of coarse elements K .

By imposing $u|_{\partial\Omega} = 0$, the weak formulation associated with (2) is to find $u \in C^0(0, T; H_0^1(\Omega)) \cap C^1(0, T; L^2(\Omega))$ such that

$$\begin{cases} (D_{tt}u, v) + (a\nabla u, \nabla v) = (f, v), \\ (u(0), v) = (g_0, v), \\ (D_t u(0), v) = (g_1, v), \end{cases} \quad (3)$$

for all $v \in H_0^1(\Omega)$. Here (\cdot, \cdot) is the standard L^2 inner product.

Let V_h be a finite dimensional subspace of $H_0^1(\Omega)$ associated with τ_h . We suppose that $u_h : [0, T] \mapsto V_h$ is a twice differentiable map with respect to t satisfying

$$\begin{cases} (D_{tt}u_h, v_h) + (a\nabla u_h, \nabla v_h) = (f, v_h), \\ (u_h(0), v_h^l) = (g_0, v_h^l), \\ (D_t u_h(0), v_h^l) = (g_1, v_h^l), \end{cases} \quad (4)$$

for any $v_h \in V_h$ and $v_h^l \in V_h$. The multiscale method that we describe in the next section relies on this weak formulation. Furthermore, if $g_{i,h}$ are the L^2 projection of g_i onto V_h for $i = 0, 1$, i.e., $(g_i - g_{i,h}, v_h^l) = 0$ for any $v_h^l \in V_h$, the stability result below can be established by slightly modifying the proof of Lemma 1 in [15].

Lemma 2.1. *Let u and u_h be the solutions to (3) and (4) respectively. Assume that $w : [0, T] \mapsto V_h$ be any function, then*

$$\|u - u_h\|_{\Omega_T} \leq C(\|u - w\|_{\Omega_T} + \|D_{tt}(u - w)\|_{L^2(L^2(\Omega))} + |g_{0,h} - w(0)|_{1,\Omega} + \|g_{1,h} - D_t w(0)\|_{L^2(\Omega)}). \quad (5)$$

We would like to note that w is usually taken to be the interpolation of u or elliptic projection of u for convergence analysis in classic finite element methods.

3. Galerkin MsFEM with limited global information

In this section, we present a framework of Galerkin MsFEM which is based on the weak formulation (4). The key here is to construct an appropriate finite-dimensional subspace of $H_0^1(\Omega)$ living in the coarse grid τ_h that is capable of representing the fine scale features in terms of limited global information. Seeking the approximate solution within this finite-dimensional space gives rise to a semi-discretized equations in the form of a system of initial value problems. Then application of proper discretization in time results in a system of algebraic equations for obtaining the solutions at various time levels.

3.1. Semi-discretization of the Galerkin MsFEM

We utilize the idea of partition of unity method (PUM) for multiple global fields to capture the fine scale information of the solution. We recall some results on PUM from [25]. The main idea of PUM is to find an accurate approximation in each “patch” and then use partition of unity functions to “paste” those patch approximations together. In context of the PUM using global fields, the span of the global fields is a patch approximation of the solution. The collection of global fields is denoted by \mathcal{G} , i.e.,

$$\mathcal{G} = \{p_i \mid j = 1, 2, \dots, N; p_1 = 1\},$$

where p_1 is a constant global field such that the Galerkin basis functions contain constant elements. With i denoting the index of a node, we set $\{\phi_i^0\}_{i=1}^I$ to be the partition unity functions, i.e., they satisfy $\sum_{i=1}^I \phi_i^0 = 1$ and $|\phi_i^0| \leq C \frac{1}{h}$. Here h is the diameter of the patches. For example, the finite element linear “pyramid” functions belong to partition unity functions. In this paper, we use the linear partition of unity functions. More properties and examples for partition of unity functions can be found in [4,25]. The Galerkin MsFEM basis functions are defined as

$$\phi_{ij} = \phi_i^0 p_j, \quad i = 1, \dots, I, \quad j = 1, \dots, N. \tag{6}$$

Setting

$$V_h^{PUM} = \text{span}\{\phi_{ij}; i = 1, \dots, I, j = 1, \dots, N\}, \tag{7}$$

the approximation is to find $u_h = \sum_{i=1}^I \sum_{j=1}^N c_{ij}(t) \phi_{ij}$ in V_h^{PUM} satisfying the weak formulation (4). We note this gives a second order system of ordinary differential equations governing $c_{ij}(t)$'s. In particular, with $U(t) = [c_{11}(t) \cdots c_{ij}(t) \cdots c_{IN}(t)]^T$, we have

$$\begin{cases} SD_{tt}U(t) + AU(t) = F, \\ U(0) = G_0, \\ D_t U(0) = G_1, \end{cases} \tag{8}$$

where S is the mass matrix whose entries are (ϕ_{ij}, ϕ_{kl}) , A is the stiffness matrix whose entries are $(a \nabla \phi_{ij}, \nabla \phi_{kl})$, F is the forcing vector whose entries are (f, ϕ_{ij}) , and G_1 and G_2 are vectors whose entries are coefficients in the projection of g_0 and g_1 onto V_h^{PUM} . Once all these in place, the global information has been captured in this system through the basis functions (6).

Remark 3.1. One example of setting up the global fields is to choose $p_1 = 1$ and $p_2 := p$ with p satisfying

$$-\nabla \cdot (a \nabla p) = f_0 \quad \text{in } \Omega, \tag{9}$$

subject to the same boundary conditions as the wave equation at initial time. Here f_0 is time-independent right-hand side and can be thought as the heterogeneous spatial part of f , e.g., $f(x, t) = f_0(x)g(t)$. If $f(x, t)$ is smooth and has no fine scale feature, we can simply take f_0 to be any smooth function because the smooth source term does not affect the fine scale feature of p . In simulations, (9) is solved on the fine scale grid by using standard finite element method, e.g., using piecewise linear basis functions. This computation of the global field is a one time overhead.

Remark 3.2. Another example is to set $p_1 = 1$, and p_2, p_3 solving the following equations

$$\begin{cases} \nabla \cdot (a \nabla p_i) = 0 \quad \text{in } \Omega, \\ p_i = x_{i-1} \quad \text{on } \partial \Omega, \end{cases} \tag{10}$$

where $x = (x_1, x_2) \in \Omega$ and $i = 2, 3$.

In this paper, we consider a special case with one non-trivial global multiscale field (in addition to a constant field). This is motivated by various flow-based upscaling studies for practical problems in reservoir simulations (see e.g., [10,16]). In this case, we would like to span 1 and a non-trivial global field p , for example, the solution of (9). It follows from the general PUM framework that basis functions in each coarse grid block are $\{\phi_i^0, \phi_i^0 p\}$ for node i . These basis functions span 1 and p along each edge of finite element K . They also span linear functions ϕ_i^0 and the functions $\phi_i^0 p$. With only one basis function for each node and preserving conformity of finite element basis functions, we have fewer basis functions that span 1 and p along each edge. These basis functions will have the least energy among all nodal functions that span 1 and p along the edges.

The construction of these multiscale basis functions is described as follows. We consider a coarse element K that has d nodes x_j . Without loss of generality, we use a rectangle element K (see Fig. 1). We denote by $\phi_i^K, i = 1, \dots, d$, functions which solve

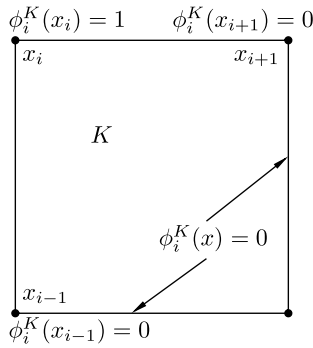


Fig. 1. Schematic description of basis function.

$$\begin{cases} -\nabla \cdot (a \nabla \phi_i^K) = 0 & \text{in } K, \\ \phi_i^K = d_i^K & \text{on } \partial K, \\ \phi_i^K(x_j) = \delta_{ij}, \end{cases} \tag{11}$$

where $\delta_{ij} = 1$ if $i = j$ and $\delta_{ij} = 0$ if $i \neq j$. Here d_i^K is the interpolation of p at two edges that have the common node x_i . Denoting these two edges by $[x_{i-1}, x_i]$ and $[x_i, x_{i+1}]$, we write

$$d_i^K(x)|_{[x_i, x_{i+1}]} = \frac{p(x) - p(x_{i+1})}{p(x_i) - p(x_{i+1})}, \quad d_i^K(x)|_{[x_{i-1}, x_i]} = \frac{p(x) - p(x_{i-1})}{p(x_i) - p(x_{i-1})}.$$

Here we have assumed $p(x_i) \neq p(x_{i+1})$. The case $p(x_i) = p(x_{i+1}) \neq 0$ and others can also be treated in similar fashion (see [16]). We take the boundary condition d_i^K to be zero along the rest of edges of the element K . The schematic description of the multiscale basis function ϕ_i^K for 2D rectangular elements is depicted in Fig. 1. The finite-dimensional subspace V_h in which the solution is sought is defined as

$$V_h = \text{span}\{\phi_i^K : i = 1, \dots, d, K \in \tau_h\}, \tag{12}$$

which is used in the following convergence analysis and the numerical experiments in Section 4.

3.2. Convergence analysis of semi-discretization Galerkin MsFEM

In this subsection, we derive an error estimate for the MsFEM solution using the multiscale basis functions (11) and finite-dimensional subspace (12). As mentioned earlier, we assume u smoothly depends on p , and thus this is a special case of (1). To be precise we have

Assumption 3.1. There exists a sufficiently smooth scalar valued function $G(\eta, t)$ ($G \in W^{1,\infty}(H^2) \cap H^2(H^2) \cap L^\infty(W^{3, \frac{2s}{s-4}}$), $s > 4$), such that for $p \in W^{1,s}$

$$\|u - G(p, t)\|_{\Omega_T} + \|D_{tt}(u - G(p, t))\|_{L^2(L^2(\Omega))} \leq \delta, \tag{13}$$

for sufficiently small δ .

This can be derived for a channelized media as it is done in [16]. Note that G is defined on a bounded domain in \mathbb{R}^2 because p is a bounded function (by using Sobolev imbedding theorem) and $[0, T]$ is bounded. Furthermore, we assume that $|\phi_i^K|_{1,K} \leq C$ for any $K \in \tau_h$. A weaker condition can also be imposed, for example, $|\phi_i^K|_{1,K} \leq Ch^{-\alpha}$ for some $\alpha > 0$, but the analysis remains the same. The following theorem establishes the convergence of the global MsFEM solution using (12) independent of small scales.

Theorem 3.1. Under Assumption 3.1 and $p \in W^{1,s}(\Omega)$ ($s > 4$),

$$\|u - u_h\|_{\Omega_T} \leq \alpha(h) + \delta + Ch^{1-\frac{2}{s}}, \tag{14}$$

C depends only on $|p|_{1,s,\Omega}$ and regularity of G , and $\alpha(h)$ is the approximation errors associated with initial conditions.

Proof. Considering V_h in (12), we take $w \in V_h$, and apply Lemma 2.1 to get

$$\|u - u_h\|_{\Omega_T} \leq C(\|u - w\|_{\Omega_T} + \|D_{tt}(u - w)\|_{L^2(L^2(\Omega))} + \alpha(h)), \tag{15}$$

Please cite this article in press as: L. Jiang et al., Analysis of global multiscale finite element methods for wave equations with continuum spatial scales, Applied Numerical Mathematics (2010), doi:10.1016/j.apnum.2010.04.011

where we assume that

$$\|g_{0,h} - w(0)\|_{1,\Omega} + \|g_{1,h} - D_t w(0)\|_{0,\Omega} \leq \alpha(h). \tag{16}$$

We note that if the initial functions g_i are smooth functions without multiscale features, we take $g_{i,h}$ as projection of g_i onto the standard finite element space (i.e., spanned by the usual polynomial basis functions) on τ_h . Otherwise, we use the projection of g_i onto V_h .

Next, by triangle inequality and applying Assumption 3.1, we estimate the first and second terms of (15):

$$\begin{aligned} \|u - w\|_{\Omega_T} + \|D_{tt}(u - w)\|_{L^2(L^2(\Omega))} &\leq \|u - G(p, t)\|_{\Omega_T} + \|G(p, t) - w\|_{\Omega_T} \\ &\quad + \|D_{tt}(u - G(p, t))\|_{L^2(L^2(\Omega))} + \|D_{tt}(G(p, t) - w)\|_{L^2(L^2(\Omega))} \\ &\leq \delta + \|G(p, t) - w\|_{\Omega_T} + \|D_{tt}(G(p, t) - w)\|_{L^2(L^2(\Omega))}. \end{aligned} \tag{17}$$

At this stage we estimate the last two terms in (17). The key idea here is to construct $w \in V_h$ that makes these terms small. In particular, we choose functions $b_i^K(t)$ so that

$$w = \sum_{K \in \tau_h} \sum_{i=1}^d b_i^K(t) \phi_i^K$$

minimizes $\|G(p, t) - w\|_{\Omega_T} + \|D_{tt}(G(p, t) - w)\|_{L^2(L^2(\Omega))}$. It is natural from the construction of w to look at the estimates over a coarse finite element K and later sum up all contributions. For this, we choose $b_i^K(t) = G(p(x_i), t)$ for $t > 0$, where x_i are nodes of K . To establish the estimate over K , we rely on perturbation of G and regularities of basis functions and the global field. Denoting \bar{p}_K the average of p over K , we write Taylor's expansion of G around \bar{p}_K

$$G(p(x), t) = G(\bar{p}_K, t) + \partial_\eta G(\bar{p}_K, t)(p(x) - \bar{p}_K) + R_2^K(x, t),$$

where

$$R_2^K(x, t) = (p(x) - \bar{p}_K)^2 \int_0^1 s \partial_\eta^2 G(p(x) + s(\bar{p}_K - p(x)), t) ds,$$

and $\partial_\eta^1 G$ and $\partial_\eta^2 G$ refer to the first and second derivative with respect to first variable $G(\eta, t)$. Using this expansion for $x = x_i$, we get

$$w|_K = \sum_{i=1}^d b_i^K(t) \phi_i^K = \sum_{i=1}^d G(p(x_i), t) \phi_i^K = I_1^K + I_2^K + I_3^K, \tag{18}$$

where using the fact that $\sum_{i=1}^d \phi_i^K = 1$,

$$\begin{aligned} I_1^K(t) &= \sum_{i=1}^d G(\bar{p}_K, t) \phi_i^K = G(\bar{p}_K, t), \\ I_2^K(x, t) &= \sum_{i=1}^d (\partial_\eta G(\bar{p}_K, t)(p(x_i) - \bar{p}_K)) \phi_i^K = \partial_\eta G(\bar{p}_K, t) \sum_{i=1}^d (p(x_i) \phi_i^K - \bar{p}_K), \\ I_3^K(x, t) &= \sum_{i=1}^d \left((p(x_i) - \bar{p}_K)^2 \phi_i^K \int_0^1 s \partial_\eta^2 G(p(x_i) + s(\bar{p}_K - p(x_i)), t) ds \right). \end{aligned} \tag{19}$$

To simplify presentation we set $\xi = (G(p(x), t) - w)$. Using the Taylor expansion, (18) and (19), we get

$$\xi|_K = \partial_\eta G(\bar{p}_K, t) \left(p(x) - \sum_{i=1}^d p(x_i) \phi_i^K \right) + R_2^K(x, t) - I_3^K(x, t), \tag{20}$$

and thus

$$D_t \xi|_K = \partial_t \partial_\eta G(\bar{p}_K, t) \left(p(x) - \sum_{i=1}^d p(x_i) \phi_i^K \right) + \partial_t R_2^K(x, t) - \partial_t I_3^K(x, t). \tag{21}$$

Notice that the partial derivative with respect to t for $R_2(x, t)$ and $I_3^K(x, t)$ only involve the global field $G(\eta, t)$. Assuming sufficient regularity of $G(\eta, t)$ (i.e., $\partial_t G(\eta, t) \in L^\infty(H^2)$) and standard interpolation estimate, we get

$$\left\| \partial_t \partial_\eta G(\bar{p}_K, t) \left(p(x) - \sum_{i=1}^d p(x_i) \phi_i^K \right) \right\|_{L^\infty(L^2(K))} \leq C \left\| p(x) - \sum_{i=1}^d p(x_i) \phi_i^K \right\|_{L^2(K)} \leq Ch^2 \|f_0\|_{L^2(K)}. \tag{22}$$

Again assuming sufficient regularity of $G(\eta, t)$ and $\|\phi_i^K\|_{1,K} \leq C$, and $|p(x) - p(y)| \leq C|x - y|^{1-\frac{2}{s}}|p|_{1,s,K}$, for $x, y \in K$, we get

$$\|\partial_t R_2^K(t)\|_{L^\infty(L^2(K))} + \|\partial_t I_3^K(t)\|_{L^\infty(L^2(K))} \leq Ch|p|_{1,4,K}^2, \tag{23}$$

where we have used Sobolev imbedding $W^{1,s} \subset W^{1,4}$ ($s > 4$). Combining (21)–(23) yields

$$\|D_t \xi\|_{L^\infty(L^2(K))} \leq C(h^2 \|f_0\|_{L^2(K)} + h|p|_{1,4,K}^2). \tag{24}$$

Furthermore, taking the gradient of (20) gives

$$\nabla \xi|_K = \partial_\eta G(\bar{p}_K, t) \left(\nabla p(x) - \sum_{i=1}^d p(x_i) \nabla \phi_i^K \right) + \nabla R_2^K(x, t) - \nabla I_3^K(x, t), \tag{25}$$

where

$$\begin{aligned} \nabla R_2^K(x, t) &= 2(p(x) - \bar{p}_K) \nabla p(x) \int_0^1 s \partial_\eta^2 G(p(x) + s(\bar{p}_K - p(x)), t) ds \\ &\quad + (p(x) - \bar{p}_K)^2 \nabla p(x) \int_0^1 (1-s) s \partial_\eta^3 G(p(x) + s(\bar{p}_K - p(x)), t) ds, \\ \nabla I_3^K(x, t) &= \sum_{i=1}^d \left((p(x_i) - \bar{p}_K)^2 \nabla \phi_i^K \int_0^1 s \partial_\eta^2 G(p(x_i) + s(\bar{p}_K - p(x_i)), t) ds \right). \end{aligned} \tag{26}$$

Using standard interpolation estimate, we get

$$\left\| \partial_\eta G(\bar{p}_K, t) \left(\nabla p(x) - \sum_{i=1}^d p(x_i) \nabla \phi_i^K \right) \right\|_{L^\infty(L^2(K))} \leq Ch \|f_0\|_{L^2(K)}. \tag{27}$$

Applying Hölder's inequality and smoothness assumption $G \in L^\infty(W^{3, \frac{2s}{s-4}})$ and $p \in W^{1,s}$ in the first equation of (26) yields

$$\begin{aligned} \|\nabla R_2^K(x, t)\|_{L^\infty(L^2(K))} &\leq Ch^{2-\frac{2}{s}} |p|_{1,s,K}^3 |G|_{L^\infty(W^{3, \frac{2s}{s-4}}(K))} + Ch^{1-\frac{2}{s}} |p|_{1,s,K} |p|_{1,2,K} \\ &\leq Ch^{2-\frac{2}{s}} |p|_{1,s,K}^3 + Ch^{1-\frac{2}{s}} |p|_{1,2,K}. \end{aligned} \tag{28}$$

Similarly, using assumption $\|\phi_i^K\|_{1,K} \leq C$ in the second equation of (26) gives

$$\|\nabla I_3^K(x, t)\|_{L^\infty(L^2(K))} \leq Ch|p|_{1,4,K}^2. \tag{29}$$

Combining (25), (27)–(29), gives

$$|\xi|_{L^\infty(H^1(K))} \leq Ch \|f_0\|_{0,K} + Ch^{2-\frac{2}{s}} |p|_{1,s,K}^3 + Ch^{1-\frac{2}{s}} |p|_{1,2,K} + Ch|p|_{1,4,K}^2. \tag{30}$$

Moreover, using similar technique as before we get

$$\|D_{tt} \xi\|_{L^2(L^2(K))} \leq Ch^2 \|f_0\|_{0,K} + Ch|p|_{1,4,K}^2, \tag{31}$$

where here we use the regularity $\partial_{tt} G \in L^2(H^2)$. Combining (24), (30), and (31) yields

$$\|\xi\|_{K_T} + \|D_{tt} \xi\|_{L^2(L^2(K))} \leq C(h \|f_0\|_{L^2(K)} + h|p|_{1,4,K}^2 + h^{2-\frac{2}{s}} |p|_{1,s,K}^3 + h^{1-\frac{2}{s}} |p|_{1,2,K}). \tag{32}$$

Summing (32) over K and taking into account (15) and (17), we have

$$\begin{aligned} \|u - u_h\|_{\Omega_T} &\leq \delta + \alpha(h) + C(h\|f_0\|_{0,\Omega} + h|p|_{1,4,\Omega}^2 + h^{1-\frac{2}{s}}|p|_{1,s,\Omega}^3 + h^{1-\frac{2}{s}}|p|_{1,2,\Omega}) \\ &\leq \delta + \alpha(h) + C(h\|f_0\|_{0,\Omega} + h|p|_{1,s,\Omega}^2 + h^{1-\frac{2}{s}}|p|_{1,s,\Omega}^3 + h^{1-\frac{2}{s}}|p|_{1,s,\Omega}) \\ &\leq \alpha(h) + \delta + Ch^{1-\frac{2}{s}}, \end{aligned} \tag{33}$$

where we have used the estimate $\sum_K Ch^{2-\frac{2}{s}}|p|_{1,s,K}^3 \leq \sum_K Ch^{2-\frac{2}{s}}|p|_{1,s,\Omega}^3 \leq Ch^{1-\frac{2}{s}}|p|_{1,s,\Omega}^3$ in the first step and Sobolev imbedding theorem is used in second step. This completes the proof. \square

Remark 3.3. If initial conditions in numerical approximation are chosen appropriately, i.e., $w(0) = g_{0,h}$ and $D_t w(0) = g_{1,h}$ in (16), then $\alpha(h) = 0$. More explanations about $\alpha(h)$ can be found on p. 219 of [17].

Remark 3.4. If $\nabla p \in L^\infty(\Omega)$, the regularity of G can be relaxed to $G \in H^2(H^2) \cap L^\infty(H^3)$ and the convergence rate would be $\delta + \alpha(h) + Ch$.

As mentioned before, we can follow the idea of Galerkin PUM to construct the basis functions incorporating multiple global fields. Given a set of global fields $\mathcal{G} = \{p_i \mid i = 1, 2, \dots, N; p_1 = 1\}$, the basis functions are defined in (6). We assume that the solution u of the wave equation (2) smoothly depends on the global fields. More precisely, we assume there exists a function $G(\eta, t) \in W^{1,\infty}(H^2) \cap H^2(H^2) \cap L^\infty(W^{3,\frac{2s}{s-4}})$, $s > 4$, $\eta \in \mathbb{R}^N$, such that

$$\|u - G(p_1, \dots, p_N, t)\|_{\Omega_T} + \|D_{tt}(u - G(p_1, \dots, p_N, t))\|_{L^2(L^2(\Omega))} \leq \delta, \tag{34}$$

where $p_i \in W^{1,s}(\Omega)$ ($s > 4$), $i = 1, 2, \dots, N$. We note that for a smooth domain, the multiple fields defined in Remark 3.2 satisfy the assumption (34) [27] where two non-trivial global fields are used. Following the procedure of the proof of Theorem 3.1, we can get the following proposition.

Proposition 3.2. Under the assumption (34) and if $s > 4$ and $\frac{2s}{s-4} > N$, we have

$$\|u - u_h\|_{\Omega_T} \leq \alpha(h) + \delta + Ch^{1-\frac{2}{s}}.$$

We would like to note that authors of [27] use a different global multiscale method to solve wave equation. Here we briefly describe their approach. Let $u_1 = p_2$ and $u_2 = p_3$, where p_2 and p_3 are the solutions of Eq. (10). Define a map $F : x \rightarrow (u_1(x), u_2(x))$, then a finite-dimensional space is defined by

$$\hat{M} = \{\varphi(F(x)) : \varphi \in X_h\},$$

where X_h is some standard finite element space, e.g., piecewise linear finite element space or weighted extended B-splines space [19]. If $u_h \in \hat{M}$, then it is shown in [27] that

$$\|u - u_h\|_{\Omega_T} \leq Ch.$$

We would like to note that the finite element meshes in [27] are curved and stretched in Euclidean coordinates, and then map the curved meshes to harmonic coordinates (u_1, u_2) via F . Moreover, the number global functions in [27] must equal to dimension of Ω . However, the finite element meshes in the Galerkin MsFEM (or PUM) approach are regular meshes (i.e., straight edges) in Euclidean coordinates, and the map F is not used explicitly to construct basis functions, and further, the number of global functions may not equal to the dimension of Ω .

3.3. Full-discretization of the Galerkin MsFEM

In the previous subsection, we have considered the semi-discretization of the wave equation (4) using the Galerkin MsFEM. Because the media has only spatial multiscales, we use the MsFEM for the space discretization and use conventional finite difference schemes to discretize the temporal variables. For the completeness, we present the time discretization of (4).

Let $u_h = \sum_{i=1}^J c_i(t)\phi_i$ be the solution of (4), where ϕ_i ($i = 1, \dots, J$) are Galerkin MsFEM basis functions defined in (11). Let $U(t) = [c_1(t), \dots, c_J(t)]^T$. Then (4) implies the following system of ordinary differential equations: Find $U(t) \in R^J$ such that

$$\begin{cases} SD_{tt}U(t) + AU(t) = F, \\ U(0) = G_0, \quad D_t U(0) = G_1, \end{cases} \tag{35}$$

where S, A, F, G_0 and G_1 have the similar definitions to (8). Using different time discretization scheme for (35) will produce different accuracy with respect to time steps.

In order to analyze the convergence rate and stability of full-discretization, we need come back to variational formulation. We introduce the following notations. Let $u_h : \{t_m\}_0^J \rightarrow V_h \subset H_0^1(\Omega)$, where J is a positive integer and V_h is the multiscale finite element space defined in (12). Let $\Delta t = \frac{T}{J}$ and u^n be the value of u at $t = n\Delta t$. We will use the following notations.

$$\begin{aligned} u^{n+\frac{1}{2}} &= \frac{u^{n+1} + u^n}{2}, \\ u^{n,\frac{1}{4}} &= \frac{1}{4}u^{n+1} + \frac{1}{2}u^n + \frac{1}{4}u^{n-1}, \\ D_t u^{\frac{1}{2}} &= \frac{u^1 - u^0}{\Delta t}, \\ D_t u^n &= \frac{u^{n+1} - u^{n-1}}{2\Delta t}, \\ D_{tt} u^n &= \frac{u^{n+1} - 2u^n + u^{n-1}}{\Delta t^2}. \end{aligned}$$

The similar notations are applied to u_h^n . The time discretization of (4) is expressed as

$$(D_{tt} u_h^m, v_h) + (a \nabla u_h^{m,\frac{1}{4}}, \nabla v_h) = (f^{m,\frac{1}{4}}, v_h), \quad \forall v_h \in V_h. \tag{36}$$

Here we assume that f is sufficiently smooth with respect to temporal variable. The scheme in (36) is unconditionally stable [15]. To avoid introducing more notations, in this subsections we assume that u_h is the solution of (36), unless otherwise is stated. Suppose w is an arbitrary map from $[0, t]$ into V_h , and $\xi = u_h - w$, $\eta = u - w$ and define consistency error

$$R^m = D_{tt} u^m - \left(\frac{1}{4} D_t u(t_{m+1}) + \frac{1}{2} D_t u(t_m) + \frac{1}{4} D_t u(t_{m-1}) \right),$$

then a straightforward calculation gives rise to

$$(D_{tt} \xi^m, v_h) + (a \nabla \xi^{m,\frac{1}{4}}, \nabla v_h) = (D_{tt} \eta^m + a \nabla \eta^{m,\frac{1}{4}} + R^m, \nabla v_h), \quad v_h \in V_h.$$

Let us define

$$\|u\|_{L^\infty_\Delta(X)} = \max_n \|u^{n+\frac{1}{2}}\|_X$$

for some normed space X (e.g., L^2 and H^1) and

$$\|u - u_h\|_{\Omega_T, \Delta} = \|D_t(u - u_h)\|_{L^\infty_\Delta(L^2(\Omega))} + \|u - u_h\|_{L^\infty_\Delta(H^1(\Omega))}.$$

By taking $v_h = D_t \xi^m$ and applying discrete Gronwall's lemma, the proof of Lemma 6 in [15] implies that

$$\|D_t \xi\|_{L^\infty_\Delta(L^2(\Omega))} + \|\xi\|_{L^\infty_\Delta(H^1(\Omega))} \leq C(\|D_t \xi^{\frac{1}{2}}\|_{0,\Omega} + \|\xi^{\frac{1}{2}}\|_{1,\Omega} + \|D_{tt} \eta\|_{0,\Omega} + \|\eta\|_{L^\infty(H^1(\Omega))} + \|D_t^4 u\|_{L^2(L^2(\Omega))} \Delta t^2).$$

Furthermore, triangle inequality gives the discrete stability estimate

$$\|u - u_h\|_{\Omega_T, \Delta} \leq C(\|D_t \xi^{\frac{1}{2}}\|_{0,\Omega} + \|\xi^{\frac{1}{2}}\|_{1,\Omega} + \|D_{tt}(u - w)\|_{0,\Omega} + \|u - w\|_{\Omega_T, \Delta} + \|D_t^4 u\|_{L^2(L^2(\Omega))} \Delta t^2).$$

By setting w to be defined in (18) and using this stability estimate with direct analogues of the arguments in the proof of Theorem 3.1, we obtain the following theorem on a spatio-temporal convergence of the global Galerkin MsFEM.

Theorem 3.3. *Let u be sufficiently smooth on t . Under assumptions in Theorem 3.1, we have*

$$\|u - u_h\|_{\Omega_T, \Delta} \leq \alpha(h) + \delta + C(h^{1-\frac{2}{s}} + \Delta t^2),$$

where $s > 4$.

It is often convenient to rewrite the system (35) as first order ordinary differential equation system

$$\begin{cases} SD_t \Theta(t) + AU(t) = F, \\ D_t U(t) - \Theta(t) = 0, \\ U(0) = G_0, \quad \Theta(0) = G_1. \end{cases} \tag{37}$$

We consider the following class of time discretization methods for (37)

$$\begin{cases} S \left(\frac{\Theta^{n+1} - \Theta^n}{\Delta t} \right) + \beta AU^{n+1} + (1 - \beta)AU^n = \beta F^{n+1} + (1 - \beta)F^n, \\ \frac{U^{n+1} - U^n}{\Delta t} - (\gamma \Theta^{n+1} + (1 - \gamma)\Theta^n) = 0, \\ U^0 = G_0, \quad \Theta^0 = G_1, \end{cases} \tag{38}$$

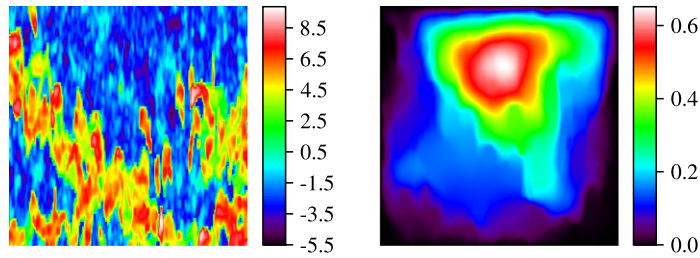


Fig. 2. Left: Log of the coefficient $a(x)$ of layer 40 of SPE 10 SPE comparative project [9], right: global field used to compute the basis functions.

where $0 \leq \beta, \gamma \leq 1$ are parameters. The semi-discretization system (37) is related to the following variational formulation with $\theta_h = D_t u_h$ (u_h is the semi-discretization solution),

$$\begin{aligned} (D_t \theta_h, v_h) + (a \nabla u_h, \nabla v_h) &= (f, v_h), \quad \forall v_h \in V_h, \\ (D_t u_h, v_h) - (\theta_h, v_h) &= 0, \quad \forall v_h \in V_h, \end{aligned}$$

and the full discretization system (38) is related to the following variational formulation

$$\begin{aligned} \left(\frac{\theta_h^{n+1} - \theta_h^n}{\Delta t}, v_h \right) + (\beta a \nabla u_h^{n+1} + (1 - \beta) a \nabla u_h^n, \nabla v_h) &= (\beta f^{n+1} + (1 - \beta) f^n, v_h), \\ \left(\frac{u_h^{n+1} - u_h^n}{\Delta t}, v_h \right) - (\gamma \theta_h^{n+1} + (1 - \gamma) \theta_h^n, v_h) &= 0, \\ (u_h^0 - g_0, v_h) &= 0, \\ (\theta_h^0 - g_1, v_h) &= 0 \end{aligned} \tag{39}$$

for $\forall v_h \in V_h$. It is known that the scheme in (39) is unconditionally stable when $\beta \geq \frac{1}{2}$ and $\gamma \geq \frac{1}{2}$. Following the standard convergence analysis [28] and the proof of Theorem 3.3, the scheme in (39) is second order accurate with respect to the time step Δt if $\beta = \frac{1}{2}$ and $\gamma = \frac{1}{2}$.

Remark 3.5. We would like to note that a weak implicit discretization is proposed in [27] and it requires less smoothness of u with respect to time. A symplectic geometric method for solving the system (37) is presented in [14] and this scheme is suitable for long-time numerical calculation.

4. Numerical results

In this section, we present a few numerical results to demonstrate the importance of incorporating global information. We will consider multiscale finite element method with limited global information presented in Section 3. All simulations are done on a domain $\Omega = [0, 1]^2$. We choose a rough coefficient $a(x)$ which induces strong non-local effects. This type of heterogeneity is presented in a benchmark test of the SPE comparative project [9] (upper Ness layers). This coefficient is highly heterogeneous, channelized, and difficult to upscale. Left plot of Fig. 2 shows the logarithmic profile of the coefficient. As can be observed, the irregular channels introduce strong non-locality across the entire domain. For these types of heterogeneities, local approaches usually fail to give an accurate results. In this experiment, we take $f = 10$, initial value $g_0 = 0$ and $g_1 = 0$. We impose zero Dirichlet boundary conditions in (2).

A natural comparison is between the local MsFEM (boundary conditions of basis equations (11) are linear) and the global MsFEM which includes some type of global information. In particular, we use the solution of the elliptic part of (2) to represent the global field. The profile of this solution is shown in the right plot of Fig. 2. We note that this practice is a one time overhead computational cost.

One drawback from using this heterogenous coefficient is that there is no known closed form true solution of (2). Our approach then is to use fully resolved numerical solution of (2) as a reference solution. Designating u_{fr} as that fully resolved solution, triangle inequality yields

$$\|u - u_h\| \leq \|u - u_{fr}\| + \|u_{fr} - u_h\|,$$

where u is the true solution of (2), u_h is the MsFEM solution, and $\|\cdot\|$ is any norms used in the previous sections. Since u_{fr} is a fully resolved approximation, the first term in the triangle inequality is of higher order compared to the second term. The second term is computable and can be quantified appropriately. The u_{fr} is computed on a mesh of 660×660 rectangles using linear finite element. On the other hand, The MsFEM solutions u_h are computed on meshes ranging from

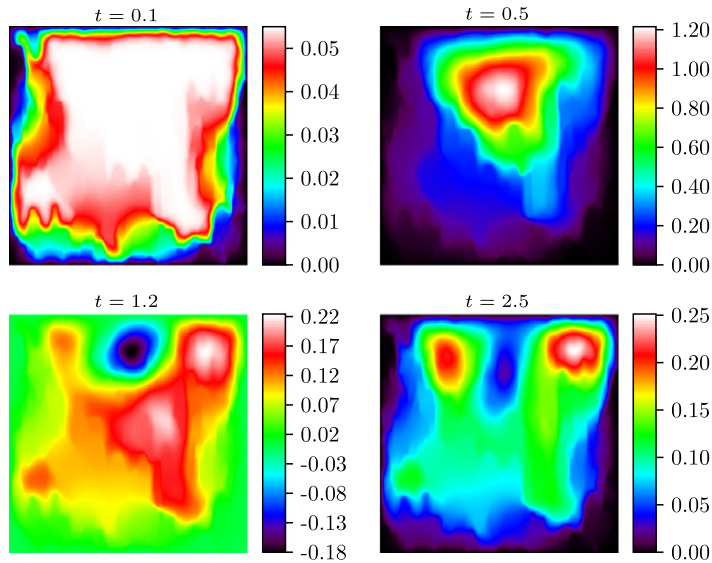


Fig. 3. Fully resolved fine scale solution at various time instances.

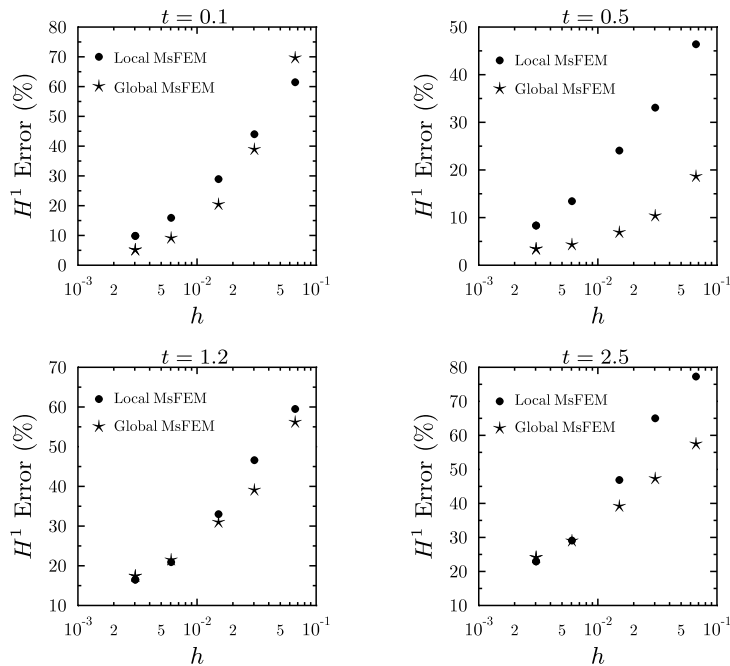


Fig. 4. Comparison of H^1 -norm error of MsFEM solutions computed at several time instances.

15×15 rectangles to 165×165 rectangles. One can immediately see several magnitude of coarsenings in the computations. In Figs. 4–7, what we mean by “Error” is the $\|u_{fr} - u_h\|$.

Computations of both u_{fr} and u_h use (39). Each of the equation in (39) is discretized using Crank–Nicholson scheme (i.e., with $\beta = \gamma = \frac{1}{2}$). In our numerical tests, we compare the solutions at several time instances. The profiles at those time levels are shown in Fig. 3.

Figs. 4 and 5 respectively give the H^1 and L^2 errors of the MsFEM solutions which are plotted against the $h = 1/N$, where N is the number of elements in either direction, ranging from 15 to 165. These errors are computed at several time instances using $\Delta t = 0.001$, both for u_{fr} and u_h . Here we compare the local MsFEM with the global MsFEM. Both figures indicate that in general the error decreases when number of elements are increased. Furthermore, the results also confirm that including global information through the multiscale basis functions does improve the accuracy of MsFEM. This is especially more significant for coarser mesh. Naturally as the mesh is refined toward reaching the fully resolved setting,

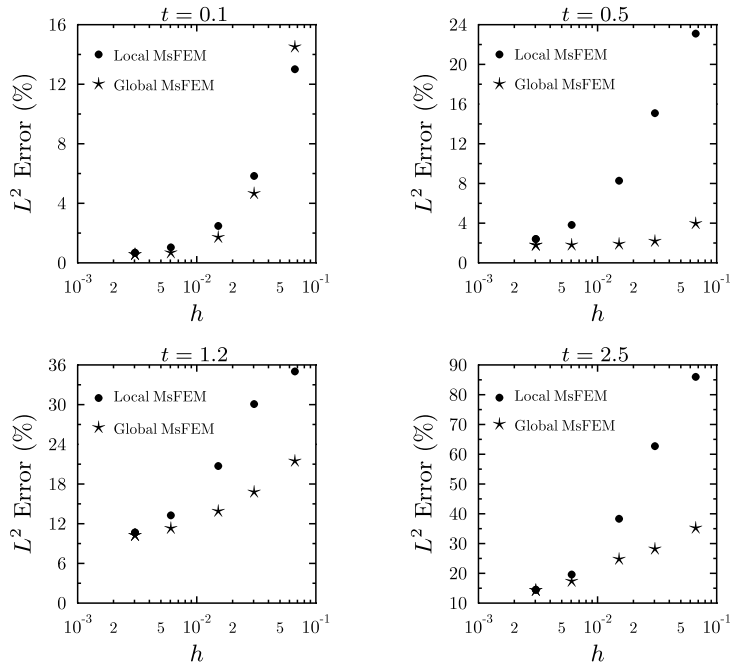


Fig. 5. Comparison of L^2 -norm error of MsFEM solutions computed at several time instances.

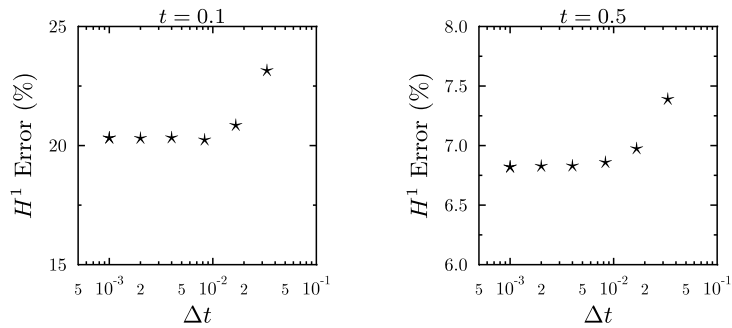


Fig. 6. H^1 -norm error of the global MsFEM solution as a function of Δt .

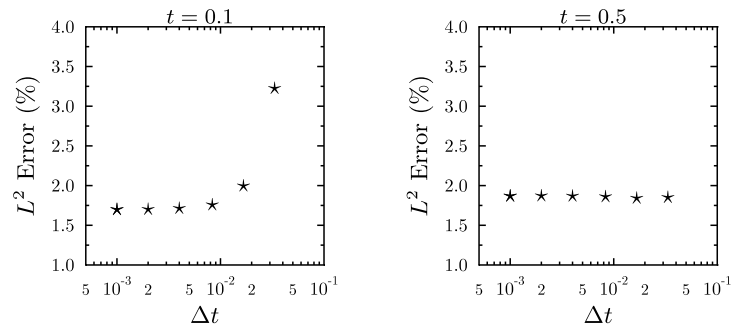


Fig. 7. L^2 -norm error of the global MsFEM solution as a function of Δt .

then the accuracy of the local and global MsFEMs is comparable. It is worth mentioning that the global MsFEM performs most accurately for computation at $t = 0.5$. This can be attributed to the similarity of the profile at this time level (see upper right plot of Fig. 3) with the global field used for the basis functions (see right plot of Fig. 2). Related to this, an improvement of accuracy can be achieved by an update of the basis functions to better reflect the dynamics at certain time

intervals. We do not explore this approach in the current investigation. Nevertheless, the results in these figures illustrate the importance of taking into consideration global information in the coarse scale computations.

Figs. 6 and 7 show the behavior of H^1 error and L^2 error of the global MsFEM solution with respect to time step Δt . Here we compute the error at $t = 0.1$ and $t = 0.5$. Again, the fully resolved solution u_{fr} is computed on 660×660 mesh and $\Delta t = 0.001$, while the global MsFEM solution is computed on 66×66 mesh with Δt ranging from $1/30$ to 0.001 . Both figures seem to show that decreasing time step does not significantly improve the accuracy of MsFEM solution as compared to the fully resolved reference. This may indicate that in fact the dominant error actually stems from the spatial heterogeneity rather than from time scale.

5. Conclusions

In this paper, we study a global numerical multiscale approach for solving wave equations with continuum spatial multiple scales. The solution is approximated on a coarse grid using multiscale basis functions. For the construction of these basis functions, we employ global functions. In particular, these global fields are defined such that the solution smoothly depends on these fields. We provide rigorous analysis for Galerkin MsFEM and present a few numerical examples. The numerical results demonstrate that the solution can be captured more accurately on a coarse grid when some global information is used.

Acknowledgements

We are grateful to reviewers who provided many insightful comments and suggestions to improve presentation of the paper. Y. Efendiev would like to acknowledge a partial support from NSF and DOE. Efendiev’s work was also partially supported by Award Number KUS-CI-016-04, made by King Abdullah University of Science and Technology (KAUST). V. Ginting’s work was supported in part by the Department of Energy (DE-NT00047-30).

Appendix A. Mixed MsFEM using multiple global fields

We present a mixed MsFEM formulation that uses multiple global fields to construct a space for the velocity. This method is mass conservative and has been applied to an elliptic equation in [2]. For simplicity, we assume zero Dirichlet boundary conditions for (2). The weak mixed formulation is to find $\{u, \sigma\} : [0, T] \rightarrow L^2(\Omega) \times H(\text{div}, \Omega)$ such that

$$\begin{cases} (D_{tt}u, w) - (\nabla \cdot \sigma, w) = (f, w) \quad \forall w \in L^2(\Omega), \\ (a^{-1}\sigma, \chi) + (u, \nabla \cdot \chi) = 0 \quad \forall \chi \in H(\text{div}, \Omega), \\ (u(0), w) = (g_0, w) \quad \forall w \in L^2(\Omega), \\ ((D_t u)(0), w) = (g_1, w) \quad \forall w \in L^2(\Omega), \\ (a^{-1}\sigma(0), \chi) = (\nabla g_0, \chi) \quad \forall \chi \in H(\text{div}, \Omega). \end{cases} \tag{40}$$

Here velocity $\sigma = a\nabla u$. For the mixed formulation, we use the global information from p_i ($i = 1, \dots, N$) described in (1). Specifically, we use $\sigma_i = a(x)\nabla p_i$ ($i = 1, \dots, N$) to build velocity basis function. We formulate the assumption as follows.

Assumption A.1. There exist functions $\sigma_1, \dots, \sigma_N$ and $A_1(t, x), \dots, A_N(t, x)$ such that $\sigma = \sum_{i=1}^N A_i(t, x)\sigma_i$, where $A_i(t, x)$ ’s are sufficiently smooth functions and $\sigma_i = a\nabla p_i$ ($i = 1, \dots, N$) solves a elliptic equation $\nabla \cdot (a\nabla p_i) = 0$ with appropriate boundary conditions.

As an example, let global fields u_1 and u_2 be defined to be the solutions of (10) and set $u = u(t, u_1, u_2)$, then

$$\sigma := a\nabla u = \sum_{i=1}^2 \frac{\partial u}{\partial u_i} a\nabla u_i := \sum_{i=1}^2 A_i(t, x)\sigma_i, \quad i = 1, 2,$$

where $A_i(t, x) = \frac{\partial u}{\partial u_i}$ and $\sigma_i = a\nabla u_i$. Provided that $f \in L^\infty(L^p(\Omega)) \cap H^1(L^p(\Omega))$, $g_1 \in W^{1,p}(\Omega)$ and $D_{tt}u(0) \in L^p(\Omega)$, then the proof of Theorem 1.1 in [27] implies that $A_i(t, x) = \frac{\partial u}{\partial u_i} \in L^\infty(W^{1,p}(\Omega))$. Consequently $A_i(t, x) \in L^2(C^{1-\frac{2}{p}}(\Omega))$ if $p > 2$ by using Sobolev embedding theorem.

To numerically approximate the mixed problem (40), we construct the basis function for σ :

$$\begin{cases} \nabla \cdot (a \nabla \phi_{ij}^K) = \frac{1}{|K|} & \text{in } K, \\ a(x) \nabla \phi_{ij}^K \cdot n_{e_l}^K = \delta_{jl} \frac{\sigma_i \cdot n_{e_l}^K}{\int_{e_l} \sigma_i \cdot n_{e_l} ds} & \text{on } \partial K, \\ \int_K \phi_{ij}^K dx = 0, \end{cases} \quad (41)$$

where $i = 1, \dots, N$ and $j = 1, \dots, d$. Here e_l denotes an edge of the finite element. Note that for each edge, we have N basis functions and we assume that $\sigma_1, \dots, \sigma_N$ are linearly independent in order to guarantee that the basis functions are linearly independent. If $\int_{e_l} \sigma_i \cdot n ds = 0$ on some e_l , we can use the local mixed MsFEM basis function [8], i.e., replace $\frac{\sigma_i \cdot n_{e_l}^K}{\int_{e_l} \sigma_i \cdot n_{e_l} ds}$ with $\frac{1}{|e_l|}$ in (41). We define $\psi_{ij}^K = a \nabla \phi_{ij}^K$ and

$$\Sigma_h = \bigoplus_K \{\psi_{ij}^K\} \subset H(\text{div}, \Omega).$$

Let $Q_h = \bigoplus_K P_0(K) \subset L^2(\Omega)$, i.e., piecewise constants, be the basis functions approximating u . Let P_h be $L^2(\Omega)$ orthogonal projection onto Q_h . Denote by R_j^K the lowest Raviart–Thomas basis function [6] associating with edge e_j of K . For $t = 0$, we define

$$\Pi_h|_K \sigma(0) = \left(\int_{e_j} a(x) \nabla g_0 \cdot n dx \right) R_j^K$$

in each element K . For $t > 0$, we define

$$\Pi_h|_K \sigma(t) = \left(\int_{e_j} A_i(t, x) \sigma_i \cdot n dx \right) \psi_{ij}^K$$

in each element K . We assume that Π_h are well defined. The numerical mixed formulation is to find $\{u_h, \sigma_h\} : (0, T] \rightarrow Q_h \times \Sigma_h$ such that

$$\begin{cases} (D_{tt} u_h, w) - (\nabla \cdot \sigma_h, w) = (f, w) \quad \forall w \in Q_h, \\ (a^{-1} \sigma_h, \chi) + (u_h, \nabla \cdot \chi) = 0 \quad \forall \chi \in \Sigma_h, \\ (u_h(0), w) = (g_0, w) \quad \forall w \in Q_h, \\ ((D_t u_h)(0), w) = (g_1, w) \quad \forall w \in Q_h, \\ (\sigma_h(0), \chi) = (\Pi_h \sigma(0), \chi) \quad \forall \chi \in RT_h^0, \end{cases} \quad (42)$$

where RT_h^0 is the lowest Raviart–Thomas space.

As for the fully discrete scheme, we may use the following scheme (see also [21,13]). The fully mixed formulation is to find $\{u_h^{n+1}, \sigma_h^{n+1}\} \in Q_h \times \Sigma_h$ such that

$$\begin{cases} (D_{tt} u_h^n, w) - (\nabla \cdot \sigma_h^n, w) = (f^n, w) \quad \forall w \in Q_h, \\ (a^{-1} \sigma_h^{n+1}, \chi) + (u_h^{n+1}, \nabla \cdot \chi) = 0 \quad \forall \chi \in \Sigma_h, \\ (u_h^0, w) = (g_0, w) \quad \forall w \in Q_h, \\ \left(\frac{2}{\Delta t} D_t u_h^{\frac{1}{2}}, w \right) - (\nabla \cdot \sigma_h^0, w) = \left(f^0 + \frac{2}{\Delta t} g_1, w \right) \quad \forall w \in Q_h, \\ (\sigma_h^0, \chi) = (\Pi_h \sigma(0), \chi) \quad \forall \chi \in RT_h^0, \end{cases} \quad (43)$$

where the difference notations are defined in Section 3.3. It is known that the scheme in (43) is conditionally stable and that the time consistency error is $O(\Delta t^2)$ if $u(t, x)$ is sufficiently smooth with respect to t (refer to [21,13]).

Remark A.1. Extensive analysis of the global mixed MsFEM has been done in [22].

References

[1] J. Aarnes, On the use of a mixed multiscale finite element method for greater flexibility and increased speed or improved accuracy in reservoir simulation, *Multiscale Model. Simul.* 2 (2004) 421–439.

- [2] J. Aarnes, Y. Efendiev, L. Jiang, Mixed multiscale finite element methods using limited global information, *Multiscale Model. Simul.* 7 (2008) 655–676.
- [3] T. Arbogast, Implementation of a locally conservative numerical subgrid upscaling scheme for two-phase Darcy flow, *Comput. Geosci.* 6 (2002) 453–481.
- [4] I. Babuška, U. Banerjee, J.E. Osborn, Survey of meshless and generalized finite element methods: A unified approach, *Acta Numer.* 12 (2003) 1–125.
- [5] N. Bleistein, J.K. Cohen, J.W. Stockwell Jr., *Mathematics of Multidimensional Seismic Imaging, Migration, and Inversion*, Interdisciplinary Applied Mathematics, vol. 13, Springer-Verlag, New York, 2001.
- [6] F. Brezzi, M. Fortin, *Mixed and Hybrid Finite Element Methods*, Springer-Verlag, Berlin, Heidelberg, New York, 1991.
- [7] Y. Chen, L.J. Durlofsky, Adaptive local-global upscaling for general flow scenarios in heterogeneous formations, *Transp. Porous Media* 62 (2006) 157–185.
- [8] Z. Chen, T.Y. Hou, A mixed multiscale finite element method for elliptic problems with oscillating coefficients, *Math. Comp.* 72 (2003) 541–576.
- [9] M. Christie, M. Blunt, Tenth SPE comparative solution project: A comparison of upscaling techniques, *SPE Reser. Eval. Eng.* 4 (2001) 308–317.
- [10] J. Chu, Y. Efendiev, V. Ginting, T. Hou, Flow based oversampling technique for multiscale finite element methods, *Advances in Water Resources* 31 (4) (2008) 599–608.
- [11] J.F. Claerbout, *Fundamentals of Geophysical Data Processing with Applications to Petroleum Prospecting*, Blackwell Scientific Publications, 1976, <http://sepwww.stanford.edu/oldreports/fgdp2/>.
- [12] J.F. Claerbout, *Imaging the Earth's Interior*, Blackwell Scientific Publications, Inc., Cambridge, MA, USA, 1985.
- [13] L. Cowsar, T. Dupont, M. Wheeler, A priori estimates for mixed finite element methods for the wave equation, *Comput. Methods Appl. Mech. Engrg.* 82 (1–3) (1990) 205–222.
- [14] Q. Dong, L. Cao, Multiscale asymptotic expansions and numerical algorithms for the wave equations of second order with rapidly oscillating coefficients, *Appl. Numer. Math.* 59 (2009) 3008–3032.
- [15] T. Dupont, L^2 estimates for Galerkin methods for second-order hyperbolic problems, *SIAM J. Numer. Anal.* 10 (1973) 880–889.
- [16] Y. Efendiev, V. Ginting, T. Hou, R. Ewing, Accurate multiscale finite element methods for two-phase flow simulations, *J. Comput. Phys.* 220 (1) (2006) 155–174.
- [17] G. Fairweather, *Finite Element Galerkin Methods for Differential Equations*, Lecture Notes in Pure and Applied Mathematics, vol. 34, Marcel Dekker, Inc., New York, Basel, 1978.
- [18] M. Gerritsen, L.J. Durlofsky, Modeling of fluid flow in oil reservoirs, *Ann. Rev. Fluid Mech.* 37 (2005) 211–238.
- [19] K. Höllig, *Finite Element Methods with B-Splines*, *Frontiers in Applied Mathematics*, vol. 26, Society for Industrial and Applied Mathematics (SIAM), Philadelphia, PA, 2003.
- [20] T.Y. Hou, X.H. Wu, A multiscale finite element method for elliptic problems in composite materials and porous media, *J. Comput. Phys.* 134 (1997) 169–189.
- [21] E. Jenkins, B. Riviere, M. Wheeler, A priori error estimates for mixed finite element approximations of the acoustic wave equation, *SIAM J. Numer. Anal.* 40 (5) (2002) 1698–1715.
- [22] L. Jiang, *Numerical multiscale finite element methods using limited global information for partial differential equations and applications*, Ph.D thesis, Texas A&M University, 2008.
- [23] L. Jiang, Y. Efendiev, V. Ginting, Multiscale methods for parabolic equations with continuum spatial scales, *DCDS-B* 8 (4) (2007) 833–859.
- [24] O. Korostyshevskaya, S.E. Minkoff, A matrix analysis of operator-based upscaling for the wave equation, *SIAM J. Numer. Anal.* 44 (2006) 586–612 (electronic).
- [25] J.M. Melenk, I. Babuška, The partition of unity finite element method: Basic theory and applications, *Comput. Methods Appl. Mech. Engrg.* 139 (1996) 289–314.
- [26] H. Owhadi, L. Zhang, Metric based up-scaling, *Comm. Pure Appl. Math.* 60 (5) (2007) 675–723.
- [27] H. Owhadi, L. Zhang, Numerical homogenization of the acoustic wave equation with a continuum of scales, *Comput. Methods Appl. Mech. Engrg.* 198 (2008) 397–406.
- [28] A. Quarteroni, A. Valli, *Numerical Approximation of Partial Differential Equations*, Springer Series in Computational Mathematics, vol. 23, 1994.
- [29] W. Symes, *Mathematics of Reflection Seismology*, Lecture Notes, 1998.
- [30] T. Vdovina, S.E. Minkoff, O. Korostyshevskaya, Operator upscaling for the acoustic wave equation, *Multiscale Model. Simul.* 4 (2005) 1305–1338 (electronic).